

Physical properties of molecular clouds in the southern outer Galaxy

J. May, H. Alvarez, and L. Bronfman

Departamento de Astronomía, Universidad de Chile, Casilla 36-D, Santiago, Chile

Received 30 January 1996 / Accepted 2 April 1997

Abstract. We have used a deep CO survey of the third galactic quadrant (May et al. 1993) to derive the physical properties of molecular clouds in the outer Galaxy. Within the range of this survey, from 194° to 270° in galactic longitude, 177 molecular clouds have been identified beyond 2 kpc from the Sun. Distances have been determined kinematically using the rotation curve of Brand (1986) with $R_\odot = 8.5$ kpc and $\Theta_\odot = 220$ km s $^{-1}$.

Power-law relations between line widths and sizes of the clouds, and between their densities and sizes have been found, although they do not fulfill exactly the requirements to be in virial equilibrium. Adopting a CO luminosity-to-H $_2$ conversion factor $X = 3.8 \cdot 10^{20}$ molecules cm $^{-2}$ (K km s $^{-1}$) $^{-1}$, the derived M_{CO} masses statistically agree with the virial masses. The derived size and mass distributions show that the clouds are smaller, less massive and with narrower lines than those in the inner Galaxy. However, the mass spectrum for the clouds in our sample with masses $\geq 2.5 \cdot 10^4 M_\odot$ has a slope -1.45 which is similar to that found for inner Galaxy clouds.

The warping and flaring of the outer molecular disk is clearly delineated.

Key words: ISM: clouds – ISM: molecules – galaxy: general – radio lines: ISM

1. Introduction

In recent years the outer Galaxy (the region beyond the solar circle) has gained attention despite the fact that a large fraction of molecular gas and regions of star formation are found in the inner Galaxy. The study of molecular clouds in the outer Galaxy is interesting for the following reasons: a) there is no distance ambiguity, that is, for a given rotation curve a unique distance can be calculated from a measured radial velocity; b) the boundaries of the molecular clouds can be determined directly from the observations because there is no source confusion nor a need of subtracting a diffuse background emission; c) the warping and flaring of the molecular disk can be studied unhindered; d) most

of the mass of the neutral interstellar medium lies in this region; e) due to differences in environmental conditions prevalent far from the galactic center, the physical properties of the molecular clouds might be different from those located inside the solar circle.

Kutner & Mead (1981) were the first to report the detection of extensive low-level CO emission from molecular clouds well outside the solar circle, from a survey of specific strips in latitude, in the longitude range $55^\circ - 95^\circ$. From the study and mapping of 32 clouds obtained from a more extensive CO survey of the third galactic quadrant, May et al. (1985; 1988) found that most of the distant CO emission falls in a pattern inclined to the galactic equator, providing the first evidence that molecular clouds without optically identified HII regions follow the galactic warp. A similar conclusion was obtained by Mead (1988) and Mead & Kutner (1988). These early studies of the warp of the molecular disk have been corroborated and extended by Wouterloot et al. (1990) using CO emission associated with selected IRAS point sources obtained by Wouterloot & Brand (1989).

Several studies of individual molecular clouds in the outer Galaxy have been carried out to derive their main physical parameters. May et al. (1985) studied 32 molecular clouds in the third galactic quadrant finding a shortage of very massive clouds ($\geq 10^6 M_\odot$) as compared with the inner Galaxy. Cohen et al. (1985) and Grabelsky et al. (1987) detected 26 clouds delineating the Carina arm beyond the solar circle. Mead & Kutner (1988) mapped 31 clouds in the first galactic quadrant outside the solar circle, reporting a lower excitation and kinetic temperatures for these objects as compared with those for the inner Galaxy. Carpenter et al. (1990) mapped 18 molecular clouds associated with bright far-infrared sources finding a tight, near-linear correlation between CO luminosity and cloud mass. Digel et al. (1990) observed 32 clouds, related to the Outer arm in the first galactic quadrant, concluding that these clouds are 4 ± 2 times less luminous in CO than those in the inner Galaxy. Sordroski (1991) studying 35 clouds located in the second, third and fourth galactic quadrants, also found that these outer Galaxy objects are under-luminous in CO by a factor of 2 - 3 as compared with the inner Galaxy ones. All the above studies have included

molecular clouds located up to 14 kpc from the galactic center. Recently, however, Brand & Wouterloot (1994) detected 11 molecular clouds with galactocentric distances larger than 18 kpc.

A deep CO survey of the third galactic quadrant with improved resolution and sensitivity has been completed by our group (May et al. 1993). While the low-resolution CO survey of the third quadrant (May et al. 1988) allowed the detection of 32 molecular clouds beyond 2 kpc from the Sun and up to 14 kpc from the galactic center, the deep CO survey of the same quadrant has allowed us to detect and map 177 molecular clouds beyond 2 kpc from the Sun and with galactocentric distances of up to 19 kpc. In spite of its low resolution the first CO survey of the third galactic quadrant led to: 1) the discovery of the Molecular Ridge in Vela (Murphy & May 1991); 2) the evidence for a warp and flaring in the molecular disk from a preliminary analysis of the data (May et al. 1985); 3) the presence of molecular counterparts to Linblad's (1967) arms and OB associations Canis Major OB2, Puppis OB2, and Puppis OB3 (Murphy 1985; May et al. 1988); and 4) the completion of the composite CO survey of the entire galactic plane (Dame et al. 1987).

The main purpose of this paper is to present the physical properties of these 177 molecular clouds and to compare these results with previous works on the outer Galaxy.

2. Observations

Observations of the $^{12}\text{CO}(J = 1 \rightarrow 0)$ line at 115 GHz were made with the Southern Millimeter-wave Telescope at Cerro Tololo, Chile. Suitable for large scale surveys, this 1.2 m diameter instrument has, at 115 GHz, a full beam-width at half maximum (FWHM) of $8.8'$ (0.147°) and a main beam efficiency of 0.82 (Cohen 1983; Bronfman et al. 1988).

The data used in this work are taken from a deep CO survey of the third galactic quadrant containing about 8000 spectra (May et al. 1993). Because of the wide strip in latitude (3°) needed to follow the emission detected in the low resolution survey, the large extent in longitude to be covered ($194^\circ - 270^\circ$), and the sensitivity required to detect the weak emission of molecular clouds in the outer Galaxy, a general sampling interval of 0.250° was used to complete the survey in a reasonable amount of time. However, where weak emission corresponding to molecular clouds farther than 12 kpc from the galactic center was detected, a sampling interval of 0.125° was used to map each individual cloud.

The observations are fully described by May et al. (1993); we include here only a brief description of them. The receiver front-end mixer was a Schottky diode cooled to 77 K with liquid nitrogen. The receiver noise temperature, excluding the atmospheric contribution, was about 380 K (SSB). Most of the observations were carried out with a 256-channel filter bank of 500 kHz channel-width, providing a 1.3 km s^{-1} velocity resolution at 115.3 GHz and a spectral range of 333 km s^{-1} . A narrow-band filter bank of the same number of channels but of 100 kHz channel-width, giving a spectral range of 66.6 km s^{-1} , was used to complete the survey in the area closest to the galactic

Table 1. Observational parameters

Galactic longitude	$194^\circ - 270^\circ$
Galactic latitude ^a	$-4^\circ - +1^\circ$
Sampling interval	0.25° (survey) 0.125° (clouds)
Telescope HPBW	0.147° ($8.8'$)
Velocity resolution	1.3 km s^{-1}
Velocity coverage	333 km s^{-1} (500 kHz) 66 km s^{-1} (100 kHz)
RMS sensitivity ($\sigma[T_A^*]$) ^b	$\leq 0.10 \text{ K}$
SSB receiver temperature	370 K
Typical SSB system temperature ^c	750 K

^a Strip inclined to the galactic plane covering at least 3° in latitude for $210^\circ \leq l \leq 270^\circ$, and only 2° in latitude for $194^\circ \leq l < 210^\circ$

^b At velocity resolution of 1.3 km s^{-1}

^c Including atmospheric and radiation losses

anticenter, and to finish the mapping of some individual clouds. Position switching was used for all the observations.

Integration time (6-12 minutes) for each spectrum was automatically set to achieve a noise level $\leq 0.10 \text{ K rms}$ at a velocity resolution of 1.3 km s^{-1} . All observations were made above 30° in elevation and under good weather conditions only. Table 1 summarizes the observational parameters.

3. Cloud properties

3.1. Individual cloud properties

Our sample consists of all the detected clouds located beyond 2 kpc from the Sun. Confusion to identify the individual clouds in the southern outer Galaxy occurs only at low velocities ($< 10 \text{ km s}^{-1}$) which correspond to local clouds at distances within 1.5 kpc of the Sun. Also, because it is not possible to obtain accurate estimates of their distances kinematically, we have considered only those clouds located beyond 2 kpc from the Sun.

Since some clouds can be quite far from the Sun and subtend a small angular size, we included in our analysis only those whose angular extension was larger than 3 beam-widths. The angular extension of each cloud was measured within the 3σ contour of the line intensity integrated over the velocity range of the cloud's CO emission. Also, clouds that were too close to the latitude boundaries of the survey were discarded to avoid errors in the determination of the sizes. Therefore, after applying to the deep CO survey such a selection criteria, we have ended up with a sample of 177 molecular clouds whose main physical properties are included in Table 2. Columns 1 and 2 correspond to the positions, in galactic coordinates, of the peak of the CO emission of each cloud. Columns 3 and 4 include V_{LSR} and ΔV_{obs} that correspond to the peak and FWHM of the gaussian fit, respectively. They have been determined from a gaussian fit to the cloud's *composite* spectrum, i.e., the sum of all spectra across the cloud's projected surface.

Table 2. Molecular clouds beyond 2 kpc from the Sun in the third galactic quadrant

l ($^{\circ}$)	b ($^{\circ}$)	V_{LSR} (km/s)	ΔV_{Obs} (km/s)	d (kpc)	r_c (pc)	M_{CO} ($10^5 M_{\odot}$)	R (kpc)
194.00	-0.50	20.9	7.7	5.9	47.5	2.80	14.3
194.25	-0.50	20.0	5.5	5.4	40.1	1.52	13.8
194.50	-1.26	14.4	3.5	3.2	14.6	0.21	11.6
194.50	-1.00	22.6	3.9	6.4	30.3	0.56	14.7
195.50	+0.00	20.4	2.6	4.9	14.8	0.19	13.3
195.75	-0.13	32.6	3.5	11.0	38.4	1.92	19.3
196.00	+0.50	20.2	3.1	4.6	25.2	0.48	12.9
197.00	+0.75	19.6	3.7	4.0	34.9	0.89	12.4
199.63	+0.25	22.6	2.8	4.1	10.1	0.09	12.4
203.00	+1.00	32.4	3.5	5.7	15.6	0.20	13.9
204.50	-0.50	26.8	4.9	4.0	16.2	0.19	12.2
204.63	+0.13	45.7	4.1	9.3	19.9	0.30	17.4
205.00	+0.75	33.3	6.5	5.3	27.0	0.62	13.5
205.25	+0.00	20.7	3.1	2.7	12.8	0.11	11.0
206.00	-0.50	20.7	3.9	2.6	10.8	0.09	10.9
206.00	+0.50	20.1	1.9	2.5	9.9	0.07	10.8
207.50	+0.25	34.4	4.7	4.9	16.1	0.23	13.1
207.75	+1.00	39.5	3.2	6.0	10.5	0.15	14.1
208.50	+0.75	39.2	5.4	5.7	17.2	0.35	13.8
208.75	-1.75	51.1	3.0	8.9	24.6	0.59	16.9
209.50	-1.25	24.9	4.9	2.9	15.3	0.14	11.2
209.50	-1.00	44.9	4.2	6.9	18.8	0.26	14.8
209.50	+0.50	29.8	4.0	3.7	21.5	0.37	11.9
210.00	-2.25	22.2	5.0	2.5	13.1	0.13	10.8
210.00	-0.75	35.0	2.7	4.6	16.9	0.28	12.7
210.13	-1.75	39.8	5.6	5.5	19.1	0.30	13.5
210.13	-1.50	37.8	5.9	5.1	15.3	0.18	13.1
210.38	+0.00	35.9	3.9	4.7	31.0	1.01	12.8
210.50	-1.50	27.6	3.5	3.3	12.6	0.09	11.4
211.25	-1.75	42.2	3.1	5.8	21.2	0.35	13.7
211.25	-1.00	43.8	3.7	6.1	10.6	0.18	14.1
211.25	-0.50	21.7	2.1	2.4	11.6	0.09	10.6
211.50	+1.00	45.4	3.5	6.4	33.4	1.19	14.3
212.25	-1.00	27.5	2.7	3.1	9.3	0.15	11.2
212.25	-1.00	44.3	4.7	6.0	32.1	1.11	13.9
213.00	+1.25	42.9	3.5	5.5	34.0	1.04	13.5
213.25	-2.00	37.1	6.8	4.5	17.3	0.21	12.5
213.75	+0.00	43.6	2.6	5.5	9.6	0.05	13.5
214.00	+0.75	44.1	5.5	5.6	30.0	0.94	13.5
214.50	-1.75	27.6	4.7	2.9	15.6	0.39	11.0
214.50	+1.00	46.0	6.1	5.9	32.2	1.13	13.7
215.00	+1.00	47.6	5.3	6.1	47.3	2.48	13.9
215.25	-0.25	29.2	3.8	3.1	22.1	0.40	11.2
215.50	-2.25	43.4	2.6	5.2	11.1	0.10	13.1
215.50	+0.25	48.7	5.7	6.2	25.3	0.52	14.0
215.75	+1.25	50.7	3.9	6.5	34.1	0.72	14.3
216.00	+0.50	45.7	3.2	5.5	13.6	0.18	13.4
216.25	+0.00	28.2	3.4	2.9	14.2	0.10	11.0
216.50	+0.50	46.7	2.5	5.7	13.9	0.13	13.5
216.50	+1.25	48.0	5.8	5.9	28.0	0.58	13.7
216.75	-1.00	31.3	4.4	3.3	13.3	0.14	11.3
217.00	+0.50	50.9	5.8	6.3	34.8	1.34	14.1
217.13	-0.13	53.8	3.6	6.9	17.0	0.22	14.6
217.25	+0.00	26.7	6.1	2.7	24.0	0.70	10.7
217.25	+0.00	27.7	3.9	2.8	18.4	0.36	10.8
217.38	-1.38	50.5	3.4	6.2	18.7	0.28	13.9
217.38	+0.25	50.5	5.6	6.2	37.3	1.55	13.9
218.00	-0.25	27.7	5.0	2.7	20.4	0.63	10.8
218.00	+0.25	22.8	3.5	2.2	16.7	0.20	10.3
218.25	-2.00	26.3	4.7	2.6	21.1	0.36	10.6
218.25	-2.00	32.3	5.0	3.3	27.2	0.72	11.3
218.75	-0.50	56.1	3.3	7.0	14.9	0.17	14.6
218.75	-0.50	59.6	2.2	7.8	16.5	0.22	15.3
219.00	-1.88	31.3	5.2	3.1	21.0	0.29	11.1
219.75	-2.00	30.9	6.0	3.0	14.0	0.21	11.0
220.25	-2.00	33.8	3.7	3.4	21.9	0.31	11.3
221.75	+0.25	63.8	4.6	8.0	13.9	0.20	15.4
222.50	-0.25	51.3	2.6	5.6	15.5	0.16	13.2
222.75	-2.00	39.7	3.6	4.0	22.3	0.29	11.7
223.25	-0.25	53.7	1.6	5.9	7.3	0.05	13.4
223.75	-2.00	63.2	3.2	7.5	16.0	0.19	14.9
228.00	-1.00	36.5	3.2	3.4	10.2	0.11	11.1
229.75	-2.50	41.3	2.6	3.9	10.9	0.12	11.4
229.88	-1.00	39.5	3.0	3.7	10.1	0.08	11.2
230.00	-1.00	39.2	3.0	3.7	19.6	0.23	11.2
230.25	-2.75	42.0	2.8	4.0	26.7	0.38	11.4
230.75	-1.25	24.4	2.5	2.1	8.3	0.05	10.0
231.13	+0.00	43.4	3.6	4.1	15.1	0.21	11.5
231.50	-1.00	43.1	7.1	4.1	30.3	0.91	11.5
232.00	+0.13	57.2	3.2	5.8	20.1	0.36	12.9
232.25	-1.00	44.6	5.8	4.2	22.7	0.37	11.6
232.75	-3.25	40.6	4.2	3.8	27.0	0.79	11.2
233.00	-1.00	47.0	6.5	4.5	24.0	0.41	11.8
233.00	-0.75	45.6	5.1	4.3	39.4	1.43	11.6
233.25	-1.75	51.6	3.4	5.0	15.2	0.16	12.2
234.00	-0.25	43.7	4.7	4.1	37.7	1.93	11.4
234.25	-0.88	76.3	4.2	8.6	36.4	0.93	15.2

Table 2. (continued)

l ($^{\circ}$)	b ($^{\circ}$)	V_{LSR} (km/s)	ΔV_{Obs} (km/s)	d (kpc)	r_c (pc)	M_{CO} ($10^5 M_{\odot}$)	R (kpc)
234.50	-0.50	28.7	3.1	2.6	9.4	0.06	10.2
234.50	-0.25	43.4	4.7	4.1	30.3	1.54	11.3
234.75	+0.50	51.9	1.9	5.0	10.7	0.09	12.1
235.00	+0.50	47.9	4.3	4.6	13.9	0.16	11.7
235.38	-1.75	80.8	3.5	9.3	34.2	0.95	15.7
235.50	+0.75	48.3	3.2	4.6	17.0	0.16	11.7
235.75	-1.50	52.6	3.8	5.1	17.7	0.19	12.1
236.38	-1.75	77.6	4.8	8.6	33.5	1.23	15.1
236.38	-1.50	29.2	3.7	2.6	15.4	0.20	10.2
236.75	-0.50	56.6	3.3	5.6	11.9	0.13	12.5
237.00	-2.00	23.2	5.5	2.1	15.0	0.19	9.8
237.13	-2.38	57.1	2.6	5.6	18.4	0.26	12.5
237.25	-1.25	74.4	7.4	8.0	29.6	1.05	14.5
237.50	-0.25	55.9	2.6	5.5	17.8	0.18	12.3
237.75	-1.00	22.4	3.2	2.0	16.1	0.26	9.7
238.38	-3.25	65.2	3.4	6.7	28.4	0.49	13.3
239.13	-3.50	23.0	3.3	2.1	13.5	0.19	9.7
239.13	-1.88	83.0	6.3	9.4	48.9	2.46	15.5
239.50	-1.88	79.9	3.3	8.8	15.3	0.41	15.0
240.25	-1.75	23.9	4.0	2.2	15.9	0.18	9.8
240.25	+0.00	68.1	3.7	7.0	19.3	0.34	13.5
240.25	+0.50	68.7	2.9	7.1	17.5	0.23	13.5
241.00	-1.25	66.1	5.7	6.8	42.4	2.76	13.2
241.75	-2.25	26.2	3.0	2.4	10.4	0.06	9.9
241.75	-0.63	68.4	5.6	7.1	49.1	3.35	13.4
242.00	-0.88	66.0	5.1	6.7	44.6	1.72	13.1
242.25	-2.75	21.5	4.3	2.0	13.4	0.19	9.6
242.25	-2.75	26.2	3.4	2.4	23.3	0.32	9.9
242.25	+0.13	69.8	4.5	7.2	41.8	1.72	13.5
242.63	+0.13	71.9	4.0	7.5	38.2	1.21	13.7
242.88	-0.50	64.3	5.7	6.5	36.8	1.58	12.9
242.88	+0.00	55.8	3.7	5.5	25.4	0.50	12.1
243.00	-3.00	22.2	3.6	2.1	16.1	0.17	9.6
243.25	-0.75	66.9	6.4	6.9	30.5	0.76	13.1
244.25	-2.50	70.4	2.6	7.3	9.0	0.13	13.4
244.50	-2.00	92.6	5.4	10.8	22.9	0.75	16.3
244.75	-0.25	62.5	4.9	6.3	15.6	0.19	12.6
246.75	-0.50	21.4	5.6	2.1	22.8	0.62	9.6
247.75	-0.75	29.9	2.7	3.0	12.8	0.09	10.0
248.00	+0.50	27.0	4.3	2.7	16.5	0.23	9.9
249.50	-3.88	89.9	3.4	10.2	25.2	0.48	15.4
249.88	-3.13	98.0	6.1	11.6	42.9	1.50	16.6
250.38	-1.00	66.4	2.6	7.0	19.3	0.20	12.7
250.63	-3.63	89.6	2.6	10.2	17.8	0.32	15.3
251.00	-2.88	29.3	2.1	3.1	7.7	0.05	10.0
251.25	-2.00	54.8	3.3	5.7	18.7	0.26	11.7
253.63	+0.00	34.7	6.1	3.8	38.1	2.64	10.2
253.75	+0.00	34.6	5.7	3.8	32.1	1.69	10.2
254.25	-1.25	36.1	4.3	4.0	23.0	0.35	10.3
254.25	-1.00	76.6	5.3	8.5	20.9	0.33	13.6
255.25	-1.00	80.1	4.2	9.0	40.1	1.18	13.9
255.38	-0.75	86.0	4.7	9.9	40.3	1.44	14.6
255.75	-1.00	35.7	3.0	4.1	15.8	0.15	10.3
256.12	-1.50	87.5	4.9	10.1	33.1	0.95	14.7
256.72	-2.00	44.4	2.6	5.0	18.6	0.28	10.8
257.00	-0.50	53.0	4.9	6.0	32.0	0.81	11.4
257.50	-2.38	93.1	6.3	11.1	36.1	1.10	15.4
257.50	-2.00	41.5	6.3	4.8	19.6	0.38	10.6
257.50	-0.25	55.5	3.7	6.3	15.4	0.19	11.6
258.50	-1.50	67.2	6.3	7.7	28.3	0.53	12.5
258.50	-1.00	81.2	6.5	9.4	34.8	0.96	13.9
259.00	-1.75	58.5	7.0	6.7	36.1	1.29	11.8
259.25	-2.50	54.5	5.6	6.3	33.0	1.16	11.5
259.75	-1.25	62.9	8.9	7.3	28.4	0.84	12.1
260.00	+0.00	60.7	6.6	7.1	27.5	0.68	12.0
260.50	-0.75	57.2	3.8	6.7	35.2	0.86	11.7

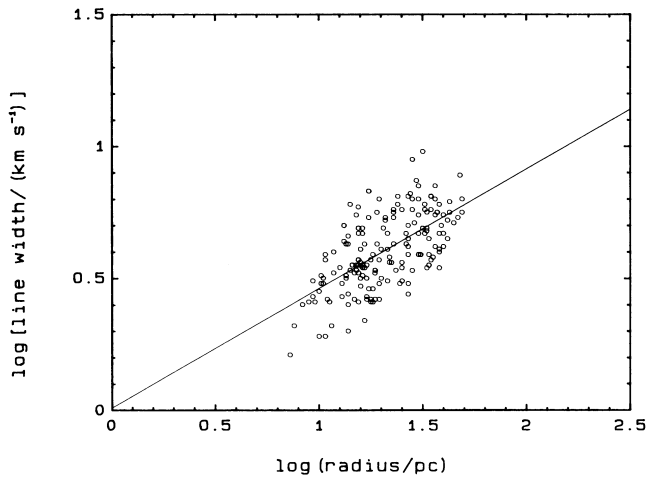


Fig. 1. Logarithm of the observed line width ΔV_{obs} (FWHM) of each cloud in Table 2 versus the logarithm of its radius r_c . The straight line shows the least-squares fit to the data given by the equation $\log \Delta V_{obs} = (0.45 \pm 0.04) \log r_c + (0.009 \pm 0.059)$

3.1.1. Distance

Since outside the solar circle there is no distance ambiguity, heliocentric distances to all 177 clouds in Table 2 (column 5) were determined kinematically, using the rotation curve of Brand (1986), and Brand and collaborators (Wouterloot & Brand 1989; Brand & Blitz 1993) with the new galactic constants, $\Theta_{\odot} = 220 \text{ km s}^{-1}$ and $R_{\odot} = 8.5 \text{ kpc}$ (Kerr & Lynden-Bell 1986). Also the rotation curve of Alvarez et al. (1990), determined from CO emission in the inner Galaxy (fourth quadrant), was used for testing purposes. We have found that both rotation curves give very close results in the outer Galaxy indicating that the flat rotation curve at 209 km s^{-1} of Alvarez et al. (1990) can be extrapolated to the whole Galaxy.

3.1.2. Radius

We define the effective radius of a cloud (column 6 in Table 2) as $\sqrt{A/\pi}$, where A is the actual projected area obtained from the angular extent of each cloud, measured from the spatial maps, and the distance. The measurements of the angular area of a cloud might be subjected to significant errors mainly because the CO emission from the clouds in the outer Galaxy is rather weak and their angular extent is small as they are usually quite far away. The angular extent of each cloud was measured within the 3σ contour of the line intensity integrated over the velocity range of the cloud's CO emission.

3.1.3. Mass

The mass, M_{CO} , of each cloud was estimated directly from its ^{12}CO luminosity on the empirically based assumption that the integrated CO line intensity is proportional to the column density of H_2 along the line of sight (e.g. Lebrun et al. 1983;

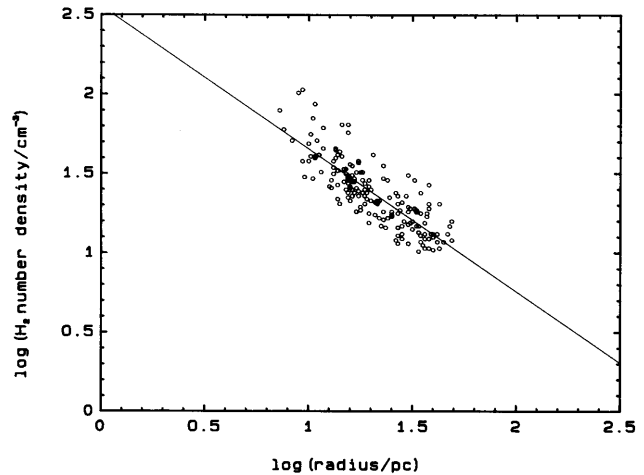


Fig. 2. Logarithm of the mean H_2 number density of each cloud in Table 2 versus the logarithm of its radius r_c . The straight line represents the least-squares fit to the data given by the equation $\log n_{\text{H}_2} = (2.55 \pm 0.06) - (0.90 \pm 0.05) \log r_c$

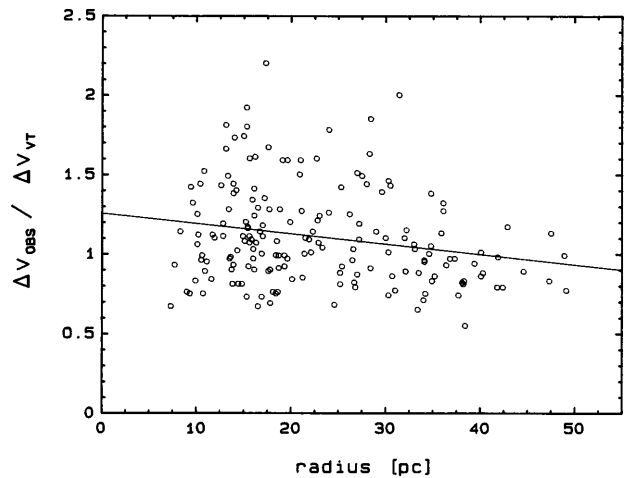


Fig. 3. Ratio of the observed ^{12}CO line width (FWHM) to the virial theorem velocity width (FWHM) versus cloud radius. The straight line represents the least-squares fit to the data given by the equation $\Delta V_{obs}/\Delta V_{VT} = (1.25 \pm 0.06) - (0.006 \pm 0.002)r_c$. Since this line is not perfectly horizontal at $\Delta V_{obs}/\Delta V_{VT} = 1$ the clouds in our sample are in *approximate* virial equilibrium only

Sanders et al. 1984; Bloemen et al. 1986). Thus, the masses were computed using the relation

$$M_{CO} = wXL_{CO}, \quad (1)$$

where w is the mean molecular weight per H_2 molecule, X is the constant ratio of H_2 column density to integrated ^{12}CO intensity, and L_{CO} is the ^{12}CO luminosity given by

$$L_{CO} = d^2 I_{CO}, \quad (2)$$

where I_{CO} is the ^{12}CO line intensity integrated over all velocities and lines of sight within the boundaries of the cloud, and d is the heliocentric distance of the cloud. In practice, I_{CO} is computed by integrating the emission over the full velocity extent of the cloud, as exhibited in the galactic latitude-velocity

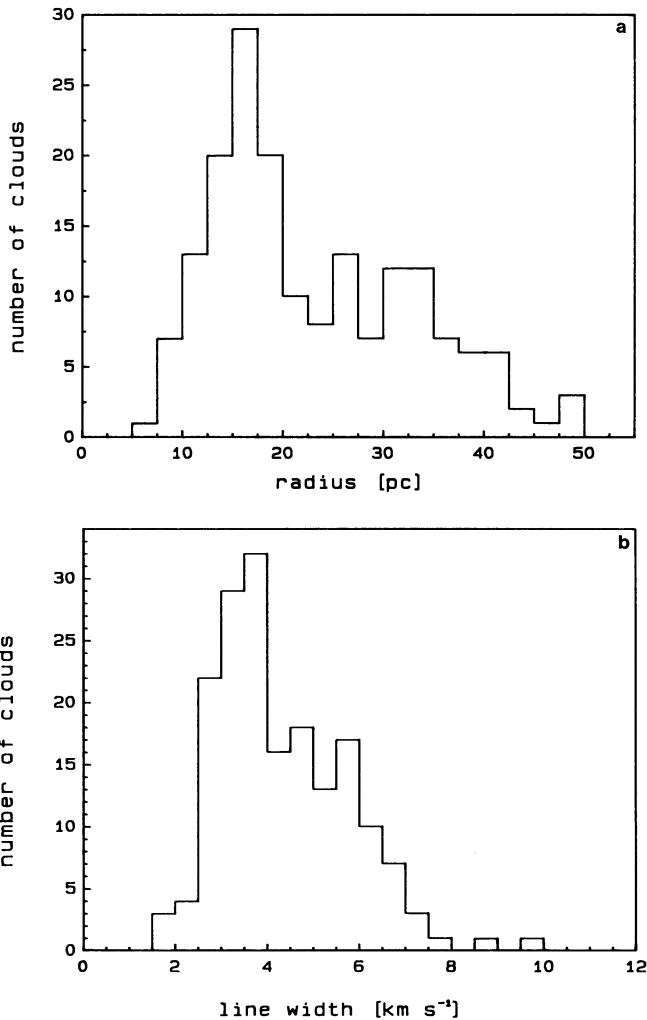


Fig. 4. **a** Size distribution and **b** line width distribution of the 177 outer Galaxy clouds for which physical properties have been derived. Our sample shows that these clouds are smaller than 50 pc with spectral lines narrower than 7.5 km s^{-1} (FWHM)

or longitude-velocity diagrams, and over the face of the cloud, defined by its 3σ contour in the spatial maps.

Several authors (Mead & Kutner 1988; Digel et al. 1990; Sodroski 1991) have claimed that X in the outer Galaxy is larger than in the inner Galaxy varying from a factor of 2 (Mead & Kutner 1988), between 2 and 3 (Sodroski 1991), to 4 ± 2 (Digel 1991). We have adopted here a value for X equal to twice the value for the inner Galaxy because it is compatible with the three estimates used for the outer Galaxy. Strong et al. (1988), through an improved analysis of the work by Bloemen et al. (1986) together with new data, derived a value of $X = (2.3 \pm 0.3) 10^{20} \text{ molecules cm}^{-2} (\text{K km s}^{-1})^{-1}$. However, this X has to be scaled down by 0.82 from the published value to account for the different calibration scale of the database from which it was derived (Bronfman et al. 1988), which gives $X = 1.9 10^{20} \text{ molecules cm}^{-2} (\text{K km s}^{-1})^{-1}$ for the inner Galaxy (Murphy & May 1991; Mauersberger et al. 1996). Therefore, assuming a mean molecular weight per H_2 molecule of 2.72 times the mass

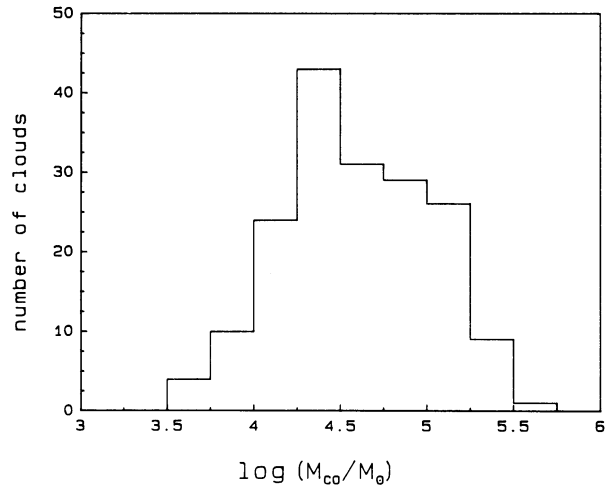


Fig. 5. Mass distribution of the 177 outer Galaxy clouds for which physical properties have been derived. The distribution shows that these clouds are less massive than $3 10^5 M_{\odot}$ and that our sample is incomplete for clouds with $M_{\text{CO}} \leq 2.5 10^4 M_{\odot}$

of the H atom to account for the He content (Allen 1973), and adopting a value of $X = 3.8 10^{20} \text{ molecules cm}^{-2} (\text{K km s}^{-1})^{-1}$ for our sample of clouds, we have

$$M_{\text{CO}} = 2.5 10^3 L_{\text{CO}}, \quad (3)$$

where M_{CO} is in M_{\odot} and L_{CO} is in $\text{K km s}^{-1} \text{ kpc}^2 \text{ deg}^2$. Note that M_{CO} denotes the *total* mass of molecular gas based on the integrated CO intensity. Table 2 (column 7) includes M_{CO} for the 177 clouds in our sample, in units of $10^5 M_{\odot}$.

For comparison the virial mass M_{VT} of each cloud was also derived using the relation

$$M_{\text{VT}} = 126 r_c (\Delta V_{\text{obs}})^2, \quad (4)$$

where M_{VT} is in solar masses, r_c is the effective radius of the cloud, in pc, and ΔV_{obs} is the HPFW of the cloud's composite spectrum, in km s^{-1} . Eq. (4) assumes: 1) the cloud is in virial equilibrium, 2) the cloud is spherical with a r^{-2} density distribution, where r is the distance from its center, 3) the observed ^{12}CO line width of the cloud is an accurate measure of the net velocity dispersion of its internal mass distribution, which is believed to be clumpy on many scales (e.g. Zuckerman & Evans 1974; Blitz & Stark 1986); or in other words, the cloud is free from magnetic or other non-gravitational forces of pressure (e.g. MacLaren et al. 1988). We are aware that magnetic forces and especially pressure terms may be important for clouds located in the galactic disk near spiral arms and regions of strong activity, like HII regions, supernovae, young stars, etc. (e.g. Myers & Goodman 1988; Elmegreen 1989; Mouschovias 1995), however, in the outer Galaxy the clouds are, in general, more isolated from their surroundings and the possible tidal effects that might take place are expected to be less important than those occurring inside the solar circle. In any case, for simplicity we have not considered in Eq. (4) the magnetic and pressure terms. We have adopted the r^{-2} density distribution considering the

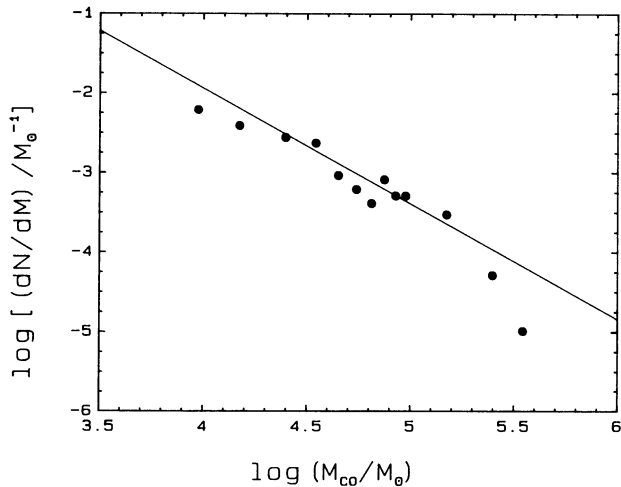


Fig. 6. Mass spectrum dN/dM versus M_{CO} for our sample of outer Galaxy clouds. The straight line represents the *weighted* least-squares fit to the data points with $M_{CO} \geq 2.5 \cdot 10^4 M_{\odot}$ and is given by the equation $\log(dN/dM) = (3.85 \pm 0.20) - (1.45 \pm 0.04) \log M_{CO}$

work of Fitzgerald et al. (1976), Dickman (1978), Snell (1981), Lorent et al. (1983), Arquilla & Goldsmith (1985) and Brand & Wouterloot (1995).

3.2. Statistical cloud properties

We have investigated some power-law relations found by several authors (e.g. Larson 1981; Myers 1983; Dame et al. 1986; Solomon et al. 1987; Sodroski 1991). Fig. 1 shows the relation between line-width and radius, r_c , for the clouds in our sample. The straight line is a least-squares fit (corr. coeff. 0.61) given by

$$\Delta V_{obs} = A r_c^{\alpha} \quad (5)$$

with $A = 1.02 \pm 0.12$ and $\alpha = 0.45 \pm 0.04$. The exponent is in agreement with previous determinations which range between 0.4 and 0.5 (e.g. Larson 1981; Dame et al. 1986; Solomon et al. 1987; Mead & Kutner 1988; Sodroski 1991).

Fig. 2 shows the relationship between the mean H_2 number density and radius for the clouds in our sample. The mean H_2 number density, n_{H_2} was computed directly from the values of r_c and M_{CO} given in Table 2, assuming a mean molecular weight per H_2 molecules of 2.72 times the mass of the H atom. A least-squares fit of

$$n_{H_2} = B r_c^{-\beta} \quad (6)$$

to the data in Fig. 2 (corr. coeff. -0.82) gives $B = 356 \pm 52$ and $\beta = 0.90 \pm 0.05$, where n_{H_2} is in cm^{-3} and r_c is in pc. The power-law exponent β is similar to the 0.94 ± 0.08 value found by Sodroski (1991) for his sample of outer Galaxy clouds.

For clouds in virial equilibrium the following condition has to be fulfilled

$$\gamma = \alpha + \beta/2 \equiv 1 \quad (7)$$

For our clouds $\gamma = 0.90 \pm 0.06$, so we will assume they are in *approximate* virial equilibrium. It should be noted that in recent years several authors (e.g. Maloney 1990; Issa et al. 1990;

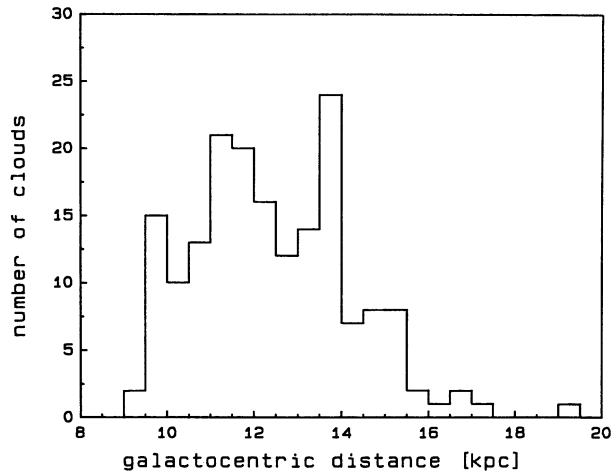


Fig. 7. Galactocentric distance distribution of the 177 outer Galaxy clouds for which physical properties have been derived. The sample appears to be incomplete for distances beyond 15.5 kpc from the galactic center

Combes 1991; Adler & Roberts 1992) have questioned whether the size-line width relationship indicates that the clouds are gravitationally bound objects.

To compare the virial masses with those computed from ^{12}CO luminosities, following Dame et al. (1986) and Sodroski (1991), we have plotted the ratio of the observed composite line widths, ΔV_{obs} , to the values expected in virial equilibrium, ΔV_{VT} , as a function of the effective radius, r_c (Fig. 3). Because of the assumptions made (3.1.3) ΔV_{VT} represents the net FWHM velocity dispersion of the internal mass distribution of a virialized spherical cloud with r^{-2} density distribution, mass M_{CO} and radius r_c , and is given by

$$\Delta V_{VT} = 0.0891(M_{CO}/r_c)^{0.5}, \quad (8)$$

where ΔV_{VT} is in km s^{-1} , M_{CO} is in M_{\odot} and r_c is in pc.

From Fig. 3 we can see that the line fitted to the data is not perfectly horizontal at $\Delta V_{obs}/\Delta V_{VT} = 1$, indicating some dependence of the ratio on the size of the clouds. This effect, that can also be seen in Fig. 3 of Sodroski (1991) and Fig. 4 of Leisawitz (1990), could be interpreted as a dependence of X on cloud size, something already commented by Scoville et al. (1987). Also Fig. 3 shows that the dispersion in the data decreases with increasing size indicating perhaps that only the larger clouds are self gravitating, that is, closer to virial equilibrium than the smaller ones. Furthermore, since the fit line is nearly horizontal at 1, the conversion factor X adopted here appears to be adequate since it yields masses which are compatible, in a statistical sense, with the virial masses derived under the assumptions described above.

The cloud size, line width and mass distribution of the clouds in our sample are shown in Figs. 4a, 4b and 5, respectively. When comparing the distribution of our clouds with those in the inner Galaxy (e.g. Dame et al. 1986; Solomon et al. 1987), it becomes evident that the clouds in the outer Galaxy are smaller (< 50 pc), less massive ($< 3 \cdot 10^5 M_{\odot}$) and with narrower lines (< 7.5 km s^{-1}). We believe this effect to be real, and not due to an

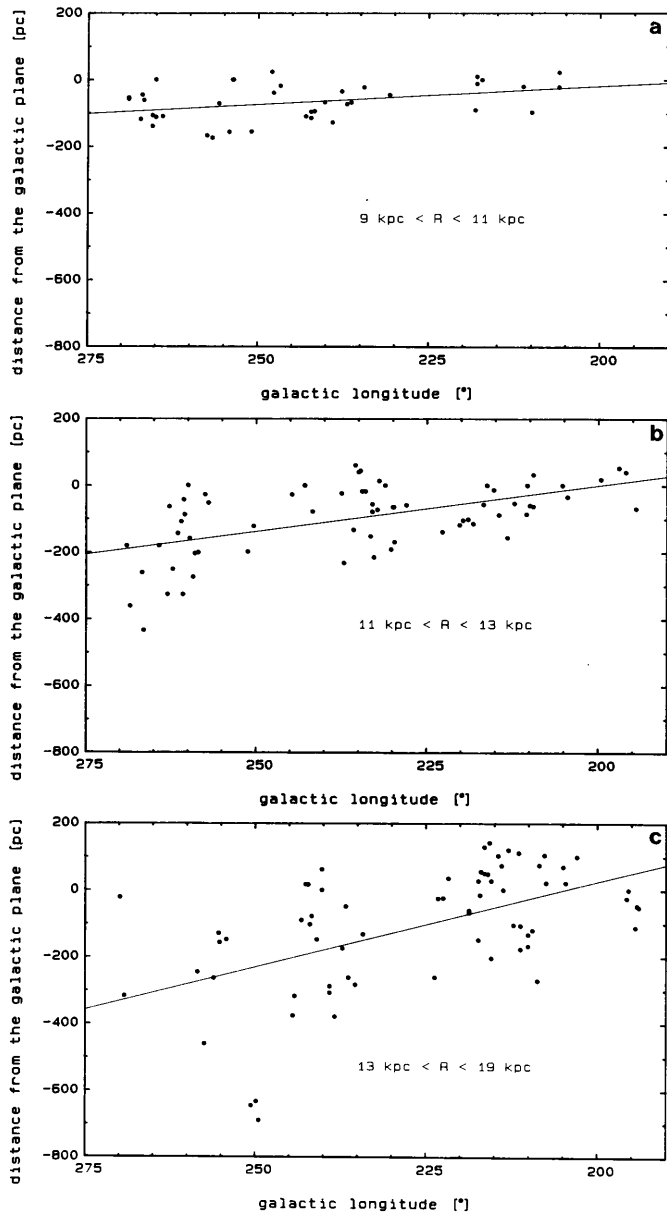


Fig. 8a–c. Distance from the galactic plane as a function of the galactic longitude for our sample of clouds. To visualize the warping and flaring of the molecular disk the ensemble of clouds has been divided in three different galactocentric distances: **a** between 9 and 11 kpc, **b** between 11 and 13 kpc, and **c** between 13 and 19 kpc. The straight line indicates roughly the inclination of the plane at each range of distances. The flaring increases from 200 pc for the nearest group up to 800 pc for the farthest

insufficient sample, as argued by Wouterloot & Brand (1995) analyzing their outer Galaxy clouds, because our ensemble of 177 clouds is large enough to provide a statistically significant result. Our results also differ from those of Sodroski (1991) who, using a sample of 32 outer Galaxy clouds, found no difference between the inner and outer Galaxy clouds. We believe our results are more reliable because Sodroski (1991) uses low resolution data (0.5°) which increases the apparent cloud's size

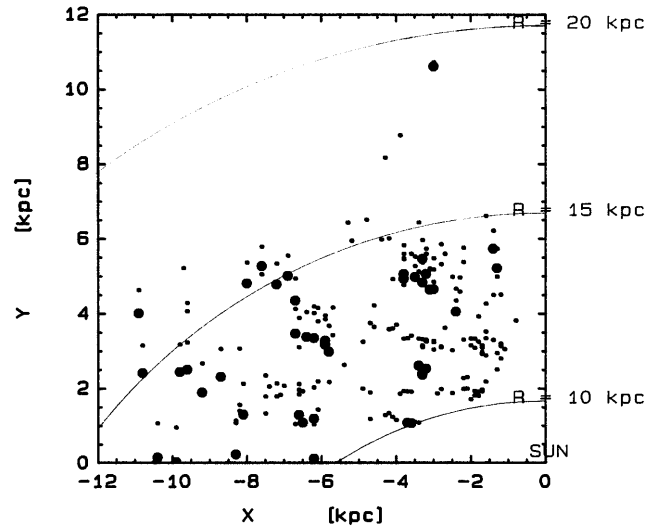


Fig. 9. Distribution of the outer Galaxy clouds from our sample projected on the galactic disk. The Sun is at $x = 0$, $y = 0$. The circle segments correspond to galactocentric distances of 10, 15, and 20 kpc, respectively. The small and large filled circles represent clouds less and more massive than $10^5 M_\odot$, respectively. No grand design spiral structure can be readily visualized from this figure

(because of the blending of clouds produced by the large synthesized low-resolution beam of the Columbia telescopes).

Fig. 6 represents the derived mass spectrum $dN/dM \propto M_{CO}^\epsilon$ for our sample of clouds, where N is the number of clouds of a given mass. In Fig. 6 we have taken bins of $10^4 M_\odot$ for $M_{CO} = 10^4 M_\odot$ to $10^5 M_\odot$, and $10^5 M_\odot$ for $M_{CO} = 10^5 M_\odot$ to $10^6 M_\odot$. The solid line corresponds to a *weighted* least-squares fit to the data points for $M_{CO} \geq 2.5 \cdot 10^4 M_\odot$ (corr. coeff. -0.95), below which the data are incomplete (Fig. 5), and is given by the equation

$$dN/dM = 7.1 \cdot 10^3 M_{CO}^{-1.45}, \quad (9)$$

where the weights are based on the number of clouds in each bin. The slope of this power-law (-1.45) is less steep than that found by Brand & Wouterloot (1995) (-1.62) for their extended sample of 112 outer Galaxy clouds taken from various authors, but it is closer to that found by Solomon & Rivolo (1989) (-1.5) for 440 clouds in the first galactic quadrant. Therefore, this similarity in the mass spectrum for clouds located inside and outside the solar circle suggests that the cloud formation mechanism is apparently independent of the galactocentric distance.

4. Distribution in the galactic disk

Once the heliocentric distance for each cloud in our sample is determined (see Sect. 3.1.1), then the corresponding galactocentric distance R can be computed. Column 8 in Table 2 displays this parameter. The galactocentric distance distribution of the 177 outer Galaxy clouds is shown in Fig. 7. The sample appears complete for distances up to 15.5 kpc from the galactic center.

Fig. 8 shows the distance from the plane, z , as a function of the galactic longitude for all our clouds. To visualize the

effect of warping and flaring of the molecular disk the ensemble of clouds has been divided in three groups depending on their galactocentric radius: a) between 9 and 11 kpc; b) between 11 and 13 kpc; and c) between 13 and 19 kpc. For our sample of clouds the maximum distance from the plane, z of about 700 pc below the plane, is found at around 250° in galactic longitude. The thickness of the molecular disk increases with galactocentric radius from 200 pc for the nearest group to 800 pc for the farthest.

The distribution of the clouds in the third quadrant projected on the galactic disk is shown in Fig. 9, where we have represented, arbitrarily, by larger filled circles the clouds which are more massive than $10^5 M_\odot$. No grand design spiral pattern can be readily visualized from the projection of the clouds on the galactic disk. A similar result has been obtained by Wouterloot et al. (1990) using CO emission associated with IRAS sources in the second and third galactic quadrants.

5. Conclusions

From the study of the physical properties of the 177 molecular clouds located in the third galactic quadrant, beyond 2 kpc from the Sun, we can conclude the following:

1. The clouds follow the size-line width and size-mean number density power-law relations found by other authors.
2. Under the assumptions made the clouds are in *approximate* virial equilibrium because they come relatively close ($\gamma = 0.90 \pm 0.06$) to fulfill the requirement of $\gamma = 1$ for clouds in virial equilibrium.
3. Adopting $X = 3.8 \cdot 10^{20}$ molecules cm^{-2} (K km s^{-1}) $^{-1}$, twice the value used for inner Galaxy clouds, the derived M_{CO} statistically agree with the computed M_{VT} .
4. The clouds are less massive, smaller and with narrower line widths than those in the inner Galaxy.
5. The mass spectrum for the clouds with $M_{CO} \geq 2.5 \cdot 10^4 M_\odot$ has a slope -1.45 , which is similar to that found for the inner Galaxy clouds (-1.50).
6. The warping and flaring of the outer molecular disk is clearly delineated.

Acknowledgements. We are grateful to Dr. M. Smith, Director of Cerro Tololo Inter-American Observatory, by supporting the operation of the 1.2 m radiotelescope. The comments and suggestions of G. Garay and L.A. Nyman are highly appreciated. We thank X. Gomez, F. MacAuliffe and F. Olmos for assistance with the data reduction, and J. Aparici, J. Garcia and G. Valladares for helping with the operation of the computing facilities. This research has been funded by FONDECYT-Chile through grant 1950570.

References

Adler D.S., Roberts W.W., 1992, ApJ 389, 95
 Allen C.W., 1973, Astrophysical Quantities. Athlone, London
 Alvarez H., May J., Bronfman L., 1990, ApJ 348, 495
 Arquilla R., Goldsmith P.F., 1985, ApJ 297, 436
 Blitz L., Stark A.A., 1986, ApJ 300, L89
 Bloemen J.B.G.M., Strong A.W., Blitz L. et al., 1986, A&A 154, 25
 Brand J., 1986, Ph.D. Thesis, University of Leiden

Brand J., Blitz L., 1993, A&A 275, 67
 Brand J., Wouterloot J.G.A., 1994, A&AS 103, 503
 Brand J., Wouterloot J.G.A., 1995, A&A 303, 851
 Bronfman L., Cohen R.S., Alvarez H., May J., Thaddeus P., 1988, ApJ 324, 248
 Carpenter J.M., Snell R.L., Schloerb F.P., 1990, ApJ 362, 147
 Cohen R.S., 1983. In: Burton W.B., Israel F.P. (eds.) Surveys of the Southern Galaxy. Reidel, Dordrecht, p. 265
 Cohen R.S., Grabelsky D.A., May J. et al., 1985, ApJ 290, L15
 Combes F., 1991, ARA&A 29, 195
 Dame T.M., Elmegreen B.G., Cohen R.S., Thaddeus P., 1986, ApJ 305, 892
 Dame T.M., Ungerechts H., Cohen R.S. et al. 1987, ApJ 322, 706
 Dickman R.L., 1978, ApJS 37, 407
 Digel S., 1991, PhD thesis, Harvard University
 Digel S., Bally J., Thaddeus P., 1990, ApJ 357, L29
 Elmegreen B.G., 1989, ApJ 338, 178
 Fitzgerald M.P., Stephens T.C., Witt A.N., 1976, ApJ 208, 709
 Grabelsky D.A., Cohen R.S., Bronfman L., Thaddeus P., May J., 1987, ApJ 315, 122
 Issa M., MacLaren I., Wolfendale A.W., 1990, ApJ 352, 132
 Kerr F.J., Lynden-Bell D., 1986, MNRAS 221, 1023
 Kutner M.L., Mead K.N., 1981, ApJ 249, L15
 Larson R.B., 1981, MNRAS 194, 809
 Lebrun F., Bennett K., Bignami G.F. et al., 1983, ApJ 274, 231
 Leisawitz D., 1990, ApJ 359, 319
 Lindblad P.O., 1967, Bull. Astron. Inst. Netherl. 19, 34
 Lorent R.B., Sandqvist A., Wootten A., 1983, ApJ 270, 620
 MacLaren I., Richardson K.M., Wolfendale A.W., 1988, ApJ 333, 821
 Maloney P., 1990, ApJ 348, L9
 Mauersberger R., Henkel C., Wielebinski R., Wiklind T., Reuter H.P., 1996, A&A 305, 421
 May J., Alvarez H., Garay G. et al., 1985. In: Shaver P., Kjär K. (eds.) ESO Conference and Workshop Proceedings No. 22, ESO-IRAM-Onsala Workshop on (Sub)-mm Astronomy. ESO, Garching, p. 245
 May J., Murphy D.C., Thaddeus P., 1988, A&AS 73, 51
 May J., Bronfman L., Alvarez H., Murphy D.C., Thaddeus P., 1993, A&AS 99, 105
 Mead K.N., 1988, ApJS 67, 149
 Mead K.N., Kutner M.L., 1988, ApJ 330, 399
 Mouschovias T.Ch., 1995, ApJ 444, L105
 Murphy D.C., 1985, PhD thesis, Massachusetts Institute of Technology
 Murphy D.C., May J., 1991, A&A 247, 202
 Myers P.C., 1983, ApJ 270, 105
 Myers P.C., Goodman A.A., 1988, ApJ 329, 392
 Sanders D.B., Solomon P.M., Scoville N.Z., 1984, ApJ 276, 182
 Scoville N.Z., Min Su Yun, Clemens D.P., Sanders D.B., Waller W.H., 1987, ApJS 63, 821
 Snell R.L., 1981, ApJS 45, 121
 Sodroski J., 1991, ApJ 366, 95
 Solomon P.M., Rivolo A.R., Barret J., Yahil A., 1987, ApJ 319, 730
 Solomon P.M., Rivolo A.R., 1989, ApJ 339, 919
 Strong A.W., Bloemen J.B.G.M., Dame T.M. et al., 1988, A&A 207, 1
 Wouterloot J.G.A., Brand J., 1989, A&AS 80, 149
 Wouterloot J.G.A., Brand J., Burton W.B., Kwee K.K., 1990, A&A 230, 21
 Wouterloot J.G.A., Brand J., 1995. In: Winniewisser G. et al. (eds.) The Physics and Chemistry of Interstellar Molecular Clouds (2nd Cologne-Zermatt Symposium), Springer, in press
 Zuckerman B., Evans N., 1974, ApJ 192, L149